

The effect of hydrodynamic-based delivery of an interleukin-13-Ig fusion gene for experimental autoimmune myocarditis in rats and its possible mechanism

Raafat Elnaggar¹, Haruo Hanawa¹, Hui Liu¹, Tsuyoshi Yoshida¹, Manabu Hayashi¹, Ritsuo Watanabe¹, Satoru Abe¹, Ken Toba¹, Kaori Yoshida¹, He Chang¹, Shiro Minagawa¹, Yuji Okura¹, Kiminori Kato¹, Makoto Kodama¹, Hiroki Maruyama², Junichi Miyazaki³, and Yoshifusa Aizawa¹

¹Division of Cardiology, Niigata University Graduate School of Medical and Dental Sciences, Niigata, Japan

²Division of Clinical Nephrology and Rheumatology, Niigata University Graduate School of Medical and Dental Sciences, Niigata, Japan

³Division of Stem Cell Regulation Research, G6, Osaka University Medical School, Suita, Japan

Running Title; IL13-Ig gene therapy in EAM

Correspondence to: H Hanawa, Division of Cardiology Niigata University Graduate School of Medical and Dental Sciences, 1-757 Asahimachi-dori, Niigata 951-8120, Japan

Key word: myocarditis, autoimmune, dilated cardiomyopathy, immune system, interleukin-13, gene therapy

Abbreviations: **ANP:** atial natriuretic peptide **Glu:** glucagons **NC:** non-cardiomyocytic **NCNI:** non-cardiomyocytic non-inflammatory **SP:** signal peptide

Total words 6471

Summary

Interleukin (IL)-13 is a pleiotropic cytokine secreted by activated Th2-T lymphocytes. Th1 cytokines are assumed to exacerbate while Th2 cytokines to ameliorate rat experimental autoimmune myocarditis (EAM). Here, we examined the effect of IL-13 on EAM using a hydrodynamic-based delivery of an IL-13-Ig and the possible mechanism of its effect. Rats were immunized on day 0 and IL-13-Ig treated rats were injected with pCAGGS-IL-13-Ig and control rats with pCAGGS-Ig on day 1 or 7. On day 17, IL-13-Ig gene therapy was effective in controlling EAM as monitored by the decreased heart weight/body weight ratio, reduced myocarditis and atrial natriuretic peptide mRNA in heart as a heart failure marker. On the basis of IL-13 receptor mRNA expression in separated cells from EAM hearts, we proposed that IL-13-Ig targeting cells were CD11b⁺ cells and non-cardiomyocytic non-inflammatory (NCNI) cells such as fibroblasts, smooth muscle or endothelial cells. IL-13-Ig inhibited expressing the genes of prostaglandin E synthase, cyclooxygenase-2, inducible nitric oxide synthase, IL-1 β and TNF α of cultivated cells from EAM hearts in contrast, while it enhanced IL-1 receptor antagonist. We concluded that IL-13-Ig ameliorates EAM and supposed that its effectiveness may be due to the influence on these immunologic molecules in CD11b⁺ and NCNI cells.

1 Introduction

Rat experimental autoimmune myocarditis (EAM) resembles giant cell myocarditis seen in humans [1]. EAM has been shown to be a T cell-mediated autoimmune myocarditis [2] and Th1 and Th2 cytokine balance is thought to be important for controlling progression and repair in EAM. Th1 and Th2 cytokines are produced at different stages of EAM [3]. mRNA for the Th1 cytokines IL-2 and IFN γ are expressed in the acute phase of EAM in the heart, with the Th2 cytokine IL-10 increasing later. Some studies have suggested that IL-10 may be effective for treatment of autoimmune diseases [4, 5] and we also reported that gene transfer of IL-10 into muscle by electroporation in vivo was effective for the treatment of EAM [6].

IL-13 is a pleiotropic cytokine secreted by activated Th2 T cells which regulates a variety of immune target cells. The human IL-13 gene is closely linked to the IL-4 gene on chromosome 5q 23-31. They are frequently co-expressed [7] and require the same receptor subunit, IL-4R α , for signal transduction [8]. Cells that express only the IL-4R, such as human T cells, respond to IL-4 but not to IL-13 [9]. Other cells that do not express the common γ chain (γ c), such as X-SCID B cells, fibroblasts and probably endothelial cells, respond to both IL-4 and IL-13 [10]. IL-13 inhibits inflammatory cytokine production by lipopolysaccharide-activated monocytes [11] and PGE₂ production by synovial fibroblasts [12] but induces IgG₄ and IgE synthesis by human B cells [13].

Gene therapy by intra-articular injections of an adenovirus producing rat IL-13 significantly ameliorates the course of rat adjuvant-induced arthritis [14]. However, IL-13 gene therapy has been investigated in only a few other autoimmune diseases and the use of a naked DNA plasmid in none. Hydrodynamics-based transfection [15] is useful for the delivery of a therapeutic protein into normal rats [16] and those with glomerulonephritis [17]. Furthermore, fusions of cytokines with Ig-Fc segments secreted as homodimers offer advantages over native cytokines, such as an extended half-life in the circulation, a characteristic of Ig, as well as a higher avidity for the ligand [18]. Here, we tested the effectiveness of IL-13-Ig gene transfer by hydrodynamic-based transfection for the suppression of EAM in rats and investigated

the possible mechanism of its effect.

2 Results

2.1 Plasma IL-13-Ig-Glu-tag protein levels

Plasma IL-13-Ig-glucagon (Glu)-tag protein levels calculated by using the Glu-tag in rats injected with pCAGGS-IL-13-Ig on day 1 increased, peaking at 48.7 ± 14.8 nmol/l (mean \pm SEM) on day 2, and gradually decreased on days 7, 12, and 17 to 7.21 ± 1.91 nmol/l, 0.55 ± 0.13 nmol/l, and 0.21 ± 0.03 nmol/l, respectively. On the other hand, the plasma Ig-Glu-tag protein levels calculated by using the Glu-tag in the pCAGGS-signal peptide (SP)-Ig control rats increased, peaking at 43.4 ± 13.5 nmol/l on day 2, and decreased on days 7, 12, 17 to 15.0 ± 3.7 nmol/l, 14.2 ± 4.85 nmol/l, and 7.59 ± 1.98 nmol/l, respectively (Fig. 1A) [19]. Plasma IL-13-Ig-glucagon (Glu)-tag protein levels calculated by using the Glu-tag in rats injected pCAGGS-IL-13-Ig on day 7 increased, peaking at 64.0 ± 7.9 nmol/l (mean \pm SEM) on day 8, and gradually decreased on days 11, 14, and 17 to 2.76 ± 0.29 nmol/l, 0.76 ± 0.14 nmol/l, and 0.25 ± 0.04 nmol/l, respectively. These levels were similar to the levels calculated by using IL-13 ELISA (Fig. 1B). It has been reported that IL-13 (5-10 ng/ml \doteq 0.4-0.8 nmol/l) suppresses the production of NO from macrophages in vitro [20]. These results indicated that a continuous effective delivery of IL-13-Ig-Glu-tag protein for more than 12 days can be achieved in rats by hydrodynamic-based transfection.

2.2 Effect of pCAGGS-rat IL-13-Ig transfer on EAM

IL-13-Ig group rats injected on day 1 (IL-13-Ig group, n=10 or SP-Ig group, n=10) or on day 7 (IL-13-Ig group, n=7 or SP-Ig group, n=7) were more active and had better appetites than Sp-Ig group rats. The heart weight/body weight ratio of the IL-13-Ig group was significantly less than that of Sp-Ig group (injection on day 1, $0.45 \pm 0.07\%$ versus $0.64 \pm 0.09\%$, $p < 0.0001$; injection on day 7, $0.43 \pm 0.14\%$ versus $0.79 \pm 0.20\%$, $p = 0.0019$) (mean \pm SD) (Fig. 2A and 2D). Many inflammatory cells and fibroblasts

had infiltrated into Sp-Ig group hearts but only a few inflammatory cells were found in the hearts of the IL-13-Ig treated group (Fig. 3). The inflammatory area of the ventricle transverse section in IL-13-Ig group was significantly smaller than the controls (injection on day 1, $1.94 \pm 1.73\%$ versus $25.1 \pm 7.3\%$, $p < 0.0001$; injection on day 7, $7.00 \pm 8.00\%$ versus $28.5 \pm 16.2\%$, $p = 0.0083$) (Fig. 2B and 2E). Gene expression of atrial natriuretic peptide (ANP) in the heart as a heart failure marker in IL-13-Ig group was significantly lower than SP-Ig group (injection on day 1, $6.03 \times 10^6 \pm 3.31 \times 10^6$ versus $51.4 \times 10^6 \pm 39.9 \times 10^6$ copy/total RNA μg , $p = 0.0038$; injection on day 7, $8.20 \times 10^7 \pm 5.11 \times 10^7$ versus $20.5 \times 10^7 \pm 5.48 \times 10^7$ copy/total RNA μg , $p = 0.0016$) (Fig. 2C and 2F). The differences of ANP mRNA between rats injected on day 1 and rats injected on day 7 were thought to be due to severer heart failure of rats injected with large volume of ringer's solution on day 7 than those on day 1.

2.3 Effect of pCAGGS-IL-13-I g transfer on infiltrating cells accumulation

In analysis of infiltrating cells in EAM hearts (Fig. 4), total cells consisting of ED1⁺, CD4⁺ and CD8⁺ cells in the heart sections were significantly fewer in the IL-13-Ig group (n=9) than in the SP-Ig group (n=9) (510 ± 104 versus 1332 ± 149 / specimen, $p < 0.0003$) (Fig. 4A). ED1⁺ cells per total cells were significantly smaller in IL-13-Ig group than in the SP-Ig group ($57.7\% \pm 2.2\%$ versus $77.1\% \pm 3.1\%$, $p = 0.0001$) (Fig. 4B). However, CD4⁺ cells or CD8⁺ per total cells were significantly larger in IL-13-Ig group (CD4⁺, $28.7\% \pm 2.0\%$ versus $15.7\% \pm 2.2\%$, $p = 0.0005$) (CD8⁺, $13.6\% \pm 0.9\%$ versus $7.2\% \pm 1.2\%$, $p = 0.0006$), respectively (Fig. 4C, D). These results demonstrated that pCAGGS-IL-13-Ig transfer could inhibit the accumulation of macrophages in the inflammatory areas of the heart compared with T cells.

2.4 IL-13R and IL-4R mRNA in separated cells from EAM hearts

We separated and purified cardiac myocytes fractions (n=5), $\alpha\beta\text{T}$ cells fractions (n=5), CD11b⁺ cells fractions (n=5) and non-cardiomyocytic non-inflammatory (NCNI) cells

fractions such as fibroblasts, smooth muscle cells or endothelial cells (n=5) from EAM hearts on day 18. NCNI cells fractions and CD11b⁺ cells fractions clearly expressed IL-13 receptor (IL-13R) α 1 mRNA in quantitative real-time PCR analysis (Fig. 5A). However, IL-13R α 1 mRNA levels expressed in $\alpha\beta$ T cells fractions were few. It suggested that there was a little contamination of NCNI cells and $\alpha\beta$ T cells didn't express IL-13R α 1. IL-4R α , which formed a heterodimer with IL-13R α 1, was detected mostly in NCNI cells fractions and $\alpha\beta$ T cells fractions, but it was detected at all cell fractions. γ c, the other molecule which could form a heterodimer with IL-4R α , was detected significantly in $\alpha\beta$ T cells fractions. IL-13R α 2, which is the decoy receptor for IL-13, was detected in NCNI cells fractions but its expression was thought to be considerably weaker than IL-13R α 1. IL-13 mRNA in EAM hearts on day 18 was not detected by RT-PCR (data not shown).

2.5 Immunologic molecules mRNA in cultivated non-cardiomyocyte cells from EAM hearts

Because we proposed that ectopic IL-13-Ig targeting cells in EAM hearts were CD11b⁺ (monocytes/macrophages) and NCNI cells (fibroblasts, smooth muscle cells or endothelial cells), we cultivated non-cardiomyocyte (NC) cells mainly consisting of fibroblasts, CD11b⁺ cells, smooth muscle cells and endothelial cells from EAM hearts (Table 1). Because genes of PGES, cyclooxygenase (Cox) 2, inducible nitric oxide synthase (iNOS), IL-1 β , TNF α and IL-1 receptor antagonist (IL-1RA) were expressed mainly by CD11b⁺ (monocytes/macrophages) or NCNI cells (data not shown), we examined the expression of these genes in cultivated NC cells. IL-13-Ig, whose concentration is similar to that in serum at early phase of EAM, significantly inhibited gene expression of PGES, Cox2, iNOS, IL-1 β and TNF α in cultivated NC cells from EAM which were stimulated with IL-1 α . IL-13-Ig almost offset the stimulation of cultivated cells by IL-1 α in the expression of these genes (Fig. 6). These phenomena were observed by IL-13-Ig whose concentration is similar to that in serum at climax of EAM (Fig. 7). In contrast, IL-13-Ig, whose concentration is similar to that in serum at early phase of EAM, significantly enhanced the expression of IL-1RA. (Fig. 6).

3 Discussion

3.1 Effect of IL-13-Ig gene transfer for EAM

In this study, we demonstrated that pCAGGS-IL-13-Ig gene transfer on day 1 or day 7 by hydrodynamic-based transfection enormously suppressed EAM in rats. It has been reported that gene delivery of recombinant IL-13 or IL-4 by using HSV-1 vectors exerted a protective effect on the development of rat EAE [21, 22]. It is widely reported that Th1 cytokines exacerbate EAE or diabetes in NOD mouse, in contrast, Th2 cytokines improve them [4, 5, 21, 22]. In this study, rats in the IL-13-Ig treatment group were very active with good appetites and only minor myocarditis. This may imply that IL-13-Ig is well-tolerated and might be expected to be useful as a drug therapy for certain autoimmune diseases. However, Afanasyeva reported that blocking IL-4 with anti-IL-4 mAb reduced the severity of mouse EAM [23]. This issue regarding IL-4, namely Th2 cytokine similar to IL-13, seems to conflict with our data and it is difficult to generalize these data rationally. Hesse reported that treatment of IL-4-neutralizing antibody over a period extending to 6 days post-immunization exacerbated the collagen-induced arthritis, but when curtailed to 2 days post-immunization, the disease was reduced [24]. Anti-IL-4 antibody therapy may act in a complicated way in the course of autoimmune disease. In addition, there may be the difference between rat EAM and mouse EAM or between IL-4 action and IL-13 action for EAM as mentioned above. Further studies are necessary to explain them clearly.

3.2 Target cells of IL-13-Ig

IL-13 is thought to act not on $\alpha\beta$ T cells but on NCNI cells and CD11b⁺ cells in EAM hearts because these cells have both IL-4R α and IL-13R α 1. Because gene transfer of IL-13-Ig on day 7, namely the time just before onset, reduced EAM significantly, we suggested that IL-13-Ig acted on these target cells in EAM hearts. It is generally agreed that IL-13 acted on monocytes and B cells, but not on T cells [25]. On the other

hand, IL-4 is thought to act on not only these cells but also $\alpha\beta$ T cells which have both IL-4R α and γc . Actually, infiltrating cells suppressed by pCAGGS-IL-13-Ig gene transfer were mainly ED1⁺ cells. ED1⁺ cells are thought to be macrophages, while IL-13R-positive NCNI cells may be fibroblasts, endothelial cells and smooth muscle cells [26]. Target cells on which IL-13 directly acts are generally supposed to be macrophages, fibroblasts, smooth muscle cells, endothelial cells and B cells [27].

3.3 Role of IL-13 targeting cells on EAM

Seventy to eighty percent of infiltrating mononuclear cells in EAM hearts are macrophages [28] and the IL-1, TNF α and iNOS produced by them play an important role in the pathogenesis of EAM [29]. On the other hand, the role of NCNI cells on EAM have not yet been fully examined. Myocardial fibroblasts in coxsackievirus B3 myocarditis produce proinflammatory cytokines [30]. In rheumatoid arthritis, fibroblasts were thought to play an important role at cartilage damage [31]. Because EAM is similar to rheumatoid arthritis, fibroblasts in EAM hearts may resemble synovial fibroblast in pathogenesis. More than 90% of the interstitial cells in the heart are fibroblasts before an inflammatory infiltration develops [32]. Fibroblasts are therefore likely to play an active role in the inflammatory reactions. PGE₂ produced by Cox2 and PGES contributes to the pathogenesis of rheumatoid arthritis, acting as a mediator of inflammation and promoting bone destruction [33].

3.4 Role of IL-13-Ig on target cells in EAM

It was well documented that IL-13 inhibited production of PGES, Cox2, iNOS and cytokines such as IL-1 or TNF α in fibroblasts or macrophages, but enhanced IL-1RA production [12, 20, 27, 34-36]. This study demonstrated that serum containing IL-13-Ig inhibited PGES, Cox2, IL-1 β , iNOS and TNF α gene expression of NC cells (mainly fibroblasts, smooth muscle cells, endothelial cells and CD11b⁺ cells) in hearts of EAM, while in contrast, it enhanced the expression of IL-1RA. Therefore, the IL-13-Ig was thought to act as an agonist at IL-13R and suppress EAM. The concentration of IL-13-

Ig used in vitro experiment was similar to that in serum at acute phase or climax of EAM. IL-13-Ig produced by hydrodynamic-based transfection was thought to influence the CD11b⁺ cells and NCNI cells in vivo as well.

Th1 cytokines play an important roles in EAM, however, because we didn't propose that $\alpha\beta$ T cells producing Th1 cytokines such as IL-2 or IFN- γ expressed IL-13R α 1 gene, we didn't analyze them. IL-13-Ig slightly decreased gene expression of IL-12 inducing Th1 cytokines in cultivated NC cells and spleen cells from EAM, but the difference was not significant (data not shown). Therefore, this study couldn't demonstrate that IL-13-Ig influenced much production of Th1 cytokines.

3.5 Hydrodynamic-based plasmid DNA delivery for various diseases

Hydrodynamic-based gene delivery can transfer into hepatocytes by retrograde blood flow from hepatic veins. Hydrodynamic-based transfection is more efficient for the production of a therapeutic protein than gene transfer into muscle by electroporation in vivo because the former method allows greater retention of synthesized proteins in the plasma than the latter [6]. Because gene transfer by a plasmid vector is easier and safer than a virus vector, it is likely that hydrodynamic-based transfection by plasmid DNA will find more applications in the future for the analysis of protein-drug effects on various diseases. On the other hand, Maruyama et al. reported high level of gene expression in the kidney cells through a hydrodynamic infusion of DNA solution to the renal vein [37]. Therefore, if modified hydrodynamic-based transfection into the hearts such as retrograde coronary venous delivery [38] is established, it may be useful for therapy in human myocarditis.

4 Materials and methods

4.1 Animals

Lewis rats were obtained from Charles River, Japan (Atsugi, Kanagawa, Japan) and were maintained in our animal facilities until they reached 8 weeks of age. Throughout

the studies, all the animals were treated in accordance with the guidelines for animal experiments of our institute.

4.2 Plasmid DNA for gene transfer

To create plasmids for the experiment, we first constructed a plasmid pCAGGS-Ig-glucagon (Glu)-tag [19] with *Swa*I and *Not*I restriction sites using PCR. The first PCR products were amplified from rat spleen cDNA using KOD Plus DNA polymerase (TOYOBO, Osaka, Japan) and the primers (5'-gaGAATTCATTTAAATgagaGCGGCCGCcgtgccagaaactgtg-3' with *Swa*I and *Not*I restriction sites and 5'-tcaaccactgcacaaaatcttgggctttaccggagagtgggagagact-3'). The final PCR product inserts were then amplified from the diluted products of the first PCR reaction with the primers (5'-gaGAATTCATTTAAATgagaGCGGCCGCcgtgccagaaactgtg-3' with *Swa*I and *Not*I restriction sites and 5'-gagagagaGAATTCcaggtattcatcaaccactgcacaaaatcttgggc-3'). These products were inserted into the pCAGGS vector using *Eco*RI sites. *Escherichia coli* JM109 competent cells were then transformed and recombinant plasmids were isolated using a Quantum Prep Plasmid Maxiprep kit (Bio-Rad Laboratories, Hercules, CA). In addition, when constructing the control plasmid, pCAGGS-SP-Ig-Glu-tag, SP of secretory leukocyte protease inhibitor cDNA was amplified from EAM heart cDNA using the primers (5'-gaGAATTCATTTAAATgaagtccagcggcctcttccc-3' and 5'-gcagcatcGCGGCCGCtcttccactccagggtgccag-3') and then inserted into a pCAGGS-Ig-Glu-tag using *Swa*I and *Not*I sites. To construct the pCAGGS-rat IL-13-Ig-Glu-tag, rat IL-13 cDNAs were amplified from phytohemagglutinin-stimulated splenocyte cDNA using the primers (5'-gaGAATTCATTTAAATggcactctgggtgactgcagtc-3' and 5'-gcagcatcGCGGCCGCgtggccatagcggaaaagttgctt-3') and then inserted into the pCAGGS-Ig-Glu-tag using *Swa*I and *Not*I sites. The recombinant plasmids were isolated as described above.

4.3 Induction of EAM

Whole cardiac myosin was prepared from the ventricular muscle of porcine hearts as previously described [39]. It was dissolved in a solution of 0.3 mol/l KCl at a concentration of 10 mg/ml and emulsified with an equal volume of complete Freund's adjuvant supplemented with 10 mg/ml of Mycobacterium tuberculosis H37RA (Difco, Detroit, Michigan). On day 0, the rats received a single immunization at 2 subcutaneous sites on the foot with a total of 0.2 ml of emulsion for each rat.

4.4 Plasmid DNA injection

Thirty four rats were divided into four groups (injection on day 1, IL-13-Ig group; n=10 or SP-Ig group; n=10; injection on day 7, IL-13-Ig group; n=7 or SP-Ig group; n=7) and were injected with 800 µg of pCAGGS-rat IL-13-Ig-Glu-tag or pCAGGS-SP-Ig-Glu-tag which was mixed with appropriate volume of ringer's solution (receiving approximately 80 ml/kg body weight) via the tail vein within 15 seconds on day 1 or day 7 [16]. Because EAM occurs from day 9 or day 10, injection of large volume after day 8 for gene transfer is thought to cause death due to heart failure. Therefore, we transferred IL-13-Ig gene on day 7 to examine the direct effects in hearts without the effects in lymphoid organs.

4.5 Plasma chimeric glucagon-tag protein measurement

Blood samples were taken on days 2, 7, 12 and 17 after gene transfer on day 1, and on days 8, 11, 14 and 17 after gene transfer on day 7. Glucagon concentrations were measured using a glucagon RIA Kit (DAIICHI RADIOISOTOPE LABS, Tokyo, Japan) [40] and rat IL-13 concentration was measured using a rat IL-13 ELISA kit (Biosource International, Camarillo, CA). Chimeric protein concentrations were calculated using glucagon-tag, (Chimeric protein concentration) (nmol/l) = (actually measured glucagon concentration) (ng/l)/(whole glucagon molecular weight), or using rat IL-13, (Chimeric protein concentration) (nmol/l) = (actually measured IL-13 concentration) (ng/l)/(whole IL-13 molecular weight).

4.6 Evaluation of histopathology

The heart weight and body weight were measured and the ratio of heart weight to body weight (g/g) was calculated. After embedding in paraffin, several transverse sections were cut from the mid-ventricle slice and stained with hematoxylin-eosin and Azan-Mallory. The myocarditis area was determined using the specimen stained with Azan-Mallory by a color image analyzer (Mac SCOPE ver. 2.6, MITANI Corporation, Japan).

4.7 Immunohistochemical staining

The hearts harvested on day 17 after the gene transfer on day 1 were embedded in Tissue-Tek O.C.T. compound (Miles Inc. Elkhart, IN) and frozen at -80°C. Transverse sections 6 µm thick were cut from the mid-ventricle slice with a cryostat and fixed in ether for 10 min. The presence of macrophages, CD4⁺ T cells and CD8⁺ T cells was examined immunohistochemically using a mouse mAb against rat macrophage (ED1, Serotec, Oxford, UK), a mouse mAb against rat CD4 (W 3/25, Serotec) or CD8 (OX-8, Serotec), biotinylated goat anti-mouse IgG₁ (Amersham, UK) and labeled streptavidin-horseradish peroxidase (Amersham). Specimens in which were observed many infiltrating cells were then selected respectively and total ED1⁺, CD4⁺ and CD8⁺ cells of IL-13 group (n=9) and Ig control group (n=9) were counted in specimens.

4.8 RNA extraction from cells separated from EAM heart

To measure mRNA of ANP as heart failure marker, total RNA was isolated from the one-third of the apical area of the heart on day 17 (injection on day 1, pCAGGS-IL-13-Ig group, n=9 or pCAGGS-SP-Ig group, n=8; injection on day 7, pCAGGS-IL-13-Ig group, n=7 or pCAGGS-SP-Ig group, n=7) using Trizol (Invitrogen, Tokyo, Japan). To evaluate target cells of IL-13, expressing IL-13R α 1 mRNA, cardiomyocytes and the other cells in hearts of EAM rats (n=5) on day 18 were isolated after collagenase perfusion treatment for 20 minutes using a Langendorff apparatus as reported

previously [41]. Briefly, isolated cells in an isotonic buffer were separated serially through stainless steel sieves into cardiomyocytes and the other cells. Because almost inflammatory cells in EAM hearts are CD11b⁺ cells and $\alpha\beta$ T cells [28], the other cells were separated into $\alpha\beta$ T cells, CD11b⁺ cells and NCNI cells such as fibroblasts, smooth muscle cells or endothelial cells by anti-PE micro beads (Miltenyi Biotec, Bergisch Gladbach, Germany) and a MACS magnetic cell sorting system (Miltenyi Biotec) using appropriate mAbs, namely PE-conjugated TCR α / β (R73) and CD11b (OX-42) (Pharmingen, San Diego, CA). The fractions of cardiomyocyte, $\alpha\beta$ T-cell, CD11b⁺ cell and NCNI cell were confirmed by analysis of specific marker gene expression, namely, α -cardiac myosin, CD3, CD11b, collagen type III, calponin and von Willebrand factor and even if the level of contamination was the highest, it was under 10% (data not shown). Total RNA was isolated from each purified cell fraction (cardiomyocytes, CD11b⁺ cells, $\alpha\beta$ T cells and NCNI cells) of EAM hearts on day 18 (acute phase n=5) using Trizol. cDNA was synthesized from 2-5 μ g of total RNA with random primers and murine Moloney leukemia virus reverse transcriptase in a final volume of 20 μ l.

4.9 Cell culture

To evaluate the effect of IL-13-Ig for the target cells in EAM heart, NC cells of EAM rat hearts on day 18 were isolated after digestion with collagenase (40 mg/100 ml) and trypsin (100 mg/100 ml) solution. The cells were cultured in 2ml of RPMI medium supplemented with 10% Fetal Calf Serum on uncoated plates. After overnight incubation, the supernatant was rinsed off and the medium was changed every 2 days, and after one week the cells achieved confluence. Sixty ng of IL-1 α was added to stimulate these cells, and then serum of a rat injected with pCAGGS-IL-13-Ig-Glu-tag (IL-13-Ig-Glu-tag protein; final concentration 2 nmol/l or 1 nmol/l) or serum of a rat injected with pCAGGS-SP-Ig-Glu-tag (Ig-Glu-tag protein; final concentration 2 nmol/l or 1 nmol/l) was added to these dishes (IL-13-Ig +IL-1 α group, SP-Ig +IL-1 α group, non-serum and non-IL-1 α group). Two nmol/l of IL-13-Ig-Glu-tag protein is similar to that in serum at acute phase of EAM rat and 1 nmol/l is similar to that in serum at

climax of EAM rat injected with pCAGGS-IL-13-Ig-Glu-tag on day 7. After 24 hours, these cells were harvested and used for quantitative real time PCR analysis to examine genes expressions of PGES, Cox2, iNOS, IL-1 β , TNF α and IL-1RA. These cultivated cells were thought to contain mainly fibroblasts, CD11b⁺ cells, smooth muscle cells and endothelial cells as determined by gene expression analysis (Table 1).

4.10 Quantitative real-time PCR analysis

To create the plasmids used for the standard, cDNAs amplified from an EAM heart using the primers (Table 2) were directly inserted into the pGEM-T vector and the recombinant plasmids were isolated after transforming *Escherichia coli* JM109 competent cells using a MagExtractor plasmid Kit (TOYOBO, Osaka, Japan). cDNA was diluted 100-fold with DNase-free water, then 5 μ l was used for real-time PCR. cDNA and diluted plasmid were amplified with the same primer used for making the plasmid and a LightCycler-FastStart DNA Master SYBR Green I kit (Roche, Indianapolis, IN). After an initial denaturation step of 10 min at 95°C, a three-step cycle procedure was used (denaturation 95°C, 10 sec, annealing 62°C, 10 sec and extension 72°C, 13 sec) for 40 cycles. LightCycler Software calculated the standard curve using five plasmid standards. The absolute copy numbers of all samples were calculated by LightCycler software using this standard curve [3].

4.11 Statistical analysis

Statistical assessment was performed by a non-paired t-test or one-way ANOVA and Bonferroni's multiple comparison test with StatView 5.0 (SAS Institute Inc.). The differences were considered significant at $p < 0.01$. Data obtained from the quantitative RT-PCR for specific cell marker and immunological molecule, immunohistochemistry data and concentration of Ig-Glu-tag protein and IL-13-Ig-Glu-tag protein are expressed as mean \pm SEM. Copy numbers of ANP mRNA, heart/body weight ratio and myocarditis area are expressed as mean \pm SD.

Acknowledgments: This study was supported in part by grants for scientific research from the Ministry of Education, Science, and Culture of Japan (No. 12670653, 14570645) and for Research on Specific Diseases of Ministry of Health, Labor and Welfare.

References

- 1 **Kodama, M., Matsumoto, Y., Fujiwara, M., Zhang, S. S., Hanawa, H., Itoh, E., Tsuda, T., Izumi, T. and Shibata, A.,** Characteristics of giant cells and factors related to the formation of giant cells in myocarditis. *Circ. Res.* 1991. **69:** 1042-1050.
- 2 **Kodama, M., Matsumoto, Y. and Fujiwara, M.,** *In vivo* lymphocyte-mediated myocardial injuries demonstrated by adoptive transfer of experimental autoimmune myocarditis. *Circulation* 1992. **85:** 1918-1926.
- 3 **Hanawa, H., Abe, S., Hayashi, M., Yoshida, T., Yoshida, K., Shiono, T., Fuse, K., Ito, M., Tachikawa, H., Kashimura, T. et al.,** Time course of gene expression in rat experimental autoimmune myocarditis. *Clin. Sci.* 2002. **103:** 623-632.
- 4 **Yang, Z., Chen, M., Wu, R., Fialkow, L. B., Bromberg, J. S., McDuffie, M., Najj, A. and Nadler, J. L.,** Suppression of autoimmune diabetes by viral IL-10 gene transfer. *J. Immunol.* 2002. **168:** 6479-6485.
- 5 **Goudy, K., Song, S., Wasserfall, C., Zhang, Y. C., Kapturczak, M., Muir, A., Powers, M., Scott-Jorgensen, M., Campbell-Thompson, M., Crawford, J. M. et al.,** Adeno-associated virus vector-mediated IL-10 gene delivery prevents type 1 diabetes in NOD mice. *Proc. Natl. Acad. Sci. U S A* 2001. **98:** 13913-13918.
- 6 **Watanabe, K., Nakazawa, M., Fuse, K., Hanawa, H., Kodama, M., Aizawa, Y., Ohnuki, T., Gejyo, F., Maruyama, H. and Miyazaki, J.,** Protection against autoimmune myocarditis by gene transfer of interleukin-10 by electroporation. *Circulation* 2001. **104:** 1098-1100.
- 7 **Dolganov, G., Bort, S., Lovett, M., Burr, J., Schubert, L., Short, D., McGurn, M., Gibson, C. and Lewis, D. B.,** Coexpression of the interleukin-13 and

- interleukin-4 genes correlates with their physical linkage in the cytokine gene cluster on human chromosome 5q23-31. *Blood* 1996. **87**: 3316-3326.
- 8 **Mueller, T. D., Zhang, J. L., Sebald, W. and Duschl, A.,** Structure, binding, and antagonists in the IL-4/IL-13 receptor system. *Biochim. Biophys. Acta* 2002. **1592**: 237-250.
- 9 **Zurawski, S. M., Vega, F., Jr., Huyghe, B. and Zurawski, G.,** Receptors for interleukin-13 and interleukin-4 are complex and share a novel component that functions in signal transduction. *Embo J.* 1993. **12**: 2663-2670.
- 10 **Callard, R. E., Matthews, D. J. and Hibbert, L.,** IL-4 and IL-13 receptors: are they one and the same? *Immunol. Today* 1996. **17**: 108-110.
- 11 **de Waal Malefyt, R., Figdor, C. G., Huijbens, R., Mohan-Peterson, S., Bennett, B., Culpepper, J., Dang, W., Zurawski, G. and de Vries, J. E.,** Effects of IL-13 on phenotype, cytokine production, and cytotoxic function of human monocytes. Comparison with IL-4 and modulation by IFN-gamma or IL-10. *J. Immunol.* 1993. **151**: 6370-6381.
- 12 **Alaeddine, N., Di Battista, J. A., Pelletier, J. P., Kiansa, K., Cloutier, J. M. and Martel-Pelletier, J.,** Inhibition of tumor necrosis factor alpha-induced prostaglandin E2 production by the antiinflammatory cytokines interleukin-4, interleukin-10, and interleukin-13 in osteoarthritic synovial fibroblasts: distinct targeting in the signaling pathways. *Arthritis Rheum.* 1999. **42**: 710-718.
- 13 **Punnonen, J., Aversa, G., Cocks, B. G., McKenzie, A. N., Menon, S., Zurawski, G., de Waal Malefyt, R. and de Vries, J. E.,** Interleukin 13 induces interleukin 4-independent IgG4 and IgE synthesis and CD23 expression by human B cells. *Proc Natl Acad Sci U S A* 1993. **90**: 3730-3734.

- 14 **Woods, J. M., Amin, M. A., Katschke, K. J., Jr., Volin, M. V., Ruth, J. H., Connors, M. A., Woodruff, D. C., Kurata, H., Arai, K., Haines, G. K., 3rd. et al,** Interleukin-13 gene therapy reduces inflammation, vascularization, and bony destruction in rat adjuvant-induced arthritis. *Hum. Gene Ther.* 2002. **13**: 381-393.
- 15 **Liu, F., Song, Y. and Liu, D.,** Hydrodynamics-based transfection in animals by systemic administration of plasmid DNA. *Gene Ther.* 1999. **6**: 1258-1266.
- 16 **Maruyama, H., Higuchi, N., Nishikawa, Y., Kameda, S., Iino, N., Kazama, J. J., Takahashi, N., Sugawa, M., Hanawa, H., Tada, N. et al.,** High-level expression of naked DNA delivered to rat liver via tail vein injection. *J. Gene Med.* 2002. **4**: 333-341.
- 17 **Higuchi, N., Maruyama, H., Kuroda, T., Kameda, S., Iino, N., Kawachi, H., Nishikawa, Y., Hanawa, H., Tahara, H., Miyazaki, J. et al.,** Hydrodynamics-based delivery of the viral interleukin-10 gene suppresses experimental crescentic glomerulonephritis in Wistar-Kyoto rats. *Gene Ther.* 2003. **10**: 1297-1310.
- 18 **Jiang, J., Yamato, E. and Miyazaki, J.,** Sustained expression of Fc-fusion cytokine following *in vivo* electroporation and mouse strain differences in expression levels. *J. Biochem. (Tokyo)* 2003. **133**: 423-427.
- 19 **Hanawa, H., Watanabe, R., Hayashi, M., Yoshida, T., Abe, S., Komura, S., Liu, H., Elnaggar, R., Chang, H., Okura, Y. et al.,** A novel method to assay proteins in blood plasma after intravenous injection of plasmid DNA. *Tohoku J. Exp. Med.* 2004. **202**: 155-161.
- 20 **Bogdan, C., Thuring, H., Dlaska, M., Rollingshoff, M. and Weiss, G.,** Mechanism of suppression of macrophage nitric oxide release by IL-13: influence of the macrophage population. *J. Immunol.* 1997. **159**: 4506-4513.

- 21 **Cash, E., Minty, A., Ferrara, P., Caput, D., Fradelizi, D. and Rott, O.,** Macrophage-inactivating IL-13 suppresses experimental autoimmune encephalomyelitis in rats. *J. Immunol.* 1994. **153:** 4258-4267.
- 22 **Furlan, R., Poliani, P. L., Marconi, P. C., Bergami, A., Ruffini, F., Adorini, L., Glorioso, J. C., Comi, G. and Martino, G.,** Central nervous system gene therapy with interleukin-4 inhibits progression of ongoing relapsing-remitting autoimmune encephalomyelitis in Biozzi AB/H mice. *Gene Ther.* 2001. **8:** 13-19.
- 23 **Afanasyeva, M., Wang, Y., Kaya, Z., Park, S., Zilliox, M. J., Schofield, B. H., Hill, S. L. and Rose, N. R.,** Experimental autoimmune myocarditis in A/J mice is an interleukin-4-dependent disease with a Th2 phenotype. *Am. J. Pathol.* 2001. **159:** 193-203.
- 24 **Hesse, M., Bayrak, S. and Mitchison, A.,** Protective major histocompatibility complex genes and the role of interleukin-4 in collagen-induced arthritis. *Eur. J. Immunol.* 1996. **26:** 3234-3237.
- 25 **Zurawski, G. and de Vries, J. E.,** Interleukin 13, an interleukin 4-like cytokine that acts on monocytes and B cells, but not on T cells. *Immunol. Today* 1994. **15:** 19-26.
- 26 **Doucet, C., Brouty-Boye, D., Pottin-Clemenceau, C., Jasmin, C., Canonica, G. W. and Azzarone, B.,** IL-4 and IL-13 specifically increase adhesion molecule and inflammatory cytokine expression in human lung fibroblasts. *Int. Immunol.* 1998. **10:** 1421-1433.
- 27 **Wynn, T. A.,** IL-13 effector functions. *Annu. Rev. Immunol.* 2003. **21:** 425-456.
- 28 **Kodama, M., Zhang, S., Hanawa, H. and Shibata, A.,** Immunohistochemical characterization of infiltrating mononuclear cells in the rat heart with experimental autoimmune giant cell myocarditis. *Clin. Exp. Immunol.* 1992. **90:** 330-335.

- 29 **Hirono, S., Islam, M. O., Nakazawa, M., Yoshida, Y., Kodama, M., Shibata, A., Izumi, T. and Imai, S.**, Expression of inducible nitric oxide synthase in rat experimental autoimmune myocarditis with special reference to changes in cardiac hemodynamics. *Circ. Res.* 1997. **80**: 11-20.
- 30 **Heim, A., Zeuke, S., Weiss, S., Ruschewski, W. and Grumbach, I. M.**, Transient induction of cytokine production in human myocardial fibroblasts by coxsackievirus B3. *Circ. Res.* 2000. **86**: 753-759.
- 31 **Morgan, M. P., Whelan, L. C., Sallis, J. D., McCarthy, C. J., Fitzgerald, D. J. and McCarthy, G. M.**, Basic calcium phosphate crystal-induced prostaglandin E2 production in human fibroblasts: role of cyclooxygenase 1, cyclooxygenase 2, and interleukin-1beta. *Arthritis Rheum.* 2004. **50**: 1642-1649.
- 32 **Eghbali, M., Czaja, M. J., Zeydel, M., Weiner, F. R., Zern, M. A., Seiffter, S. and Blumenfeld, O. O.**, Collagen chain mRNAs in isolated heart cells from young and adult rats. *J. Mol. Cell. Cardiol.* 1988. **20**: 267-276.
- 33 **Westman, M., Korotkova, M., af Klint, E., Stark, A., Audoly, L. P., Klareskog, L., Ulfgren, A. K. and Jakobsson, P. J.**, Expression of microsomal prostaglandin E synthase 1 in rheumatoid arthritis synovium. *Arthritis Rheum.* 2004. **50**: 1774-1780.
- 34 **Gabay, C., Porter, B., Guenette, D., Billir, B. and Arend, W. P.**, Interleukin-4 (IL 4) and IL-13 enhance the effect of IL-1beta on production of IL-1 receptor antagonist by human primary hepatocytes and hepatoma HepG2 cells: differential effect on C-reactive protein production. *Blood* 1999. **93**: 1299-1307.
- 35 **Kolios, G., Rooney, N., Murphy, C. T., Robertson, D. A. and Westwick, J.**, Expression of inducible nitric oxide synthase activity in human colon epithelial cells: modulation by T lymphocyte derived cytokines. *Gut* 1998. **43**: 56-63.

- 36 **Saito, A., Okazaki, H., Sugawara, I., Yamamoto, K. and Takizawa, H.,** Potential action of IL-4 and IL-13 as fibrogenic factors on lung fibroblasts in vitro. *Int. Arch. Allergy. Immunol.* 2003. **132:** 168-176.
- 37 **Maruyama, H., Higuchi, N., Nishikawa, Y., Hirahara, H., Iino, N., Kameda, S., Kawachi, H., Yaoita, E., Gejyo, F. and Miyazaki, J.,** Kidney-targeted naked DNA transfer by retrograde renal vein injection in rats. *Hum. Gene Ther.* 2002. **13:** 455-468.
- 38 **Hou, D., Maclaughlin, F., Thiesse, M., Panchal, V. R., Bekkers, B. C., Wilson, E. A., Rogers, P. I., Coleman, M. C. and March, K. L.,** Widespread regional myocardial transfection by plasmid encoding Del-1 following retrograde coronary venous delivery. *Catheter. Cardiovasc. Interv.* 2003. **58:** 207-211.
- 39 **Kodama, M., Matsumoto, Y., Fujiwara, M., Masani, F., Izumi, T. and Shibata, A.,** A novel experimental model of giant cell myocarditis induced in rats by immunization with cardiac myosin fraction. *Clin. Immunol. Immunopathol.* 1990. **57:** 250-262.
- 40 **Nishino, T., Kodaira, T., Shin, S., Imagawa, K., Shima, K., Kumahara, Y., Yanaihara, C. and Yanaihara, N.,** Glucagon radioimmunoassay with use of antiserum to glucagon C-terminal fragment. *Clin. Chem.* 1981. **27:** 1690-1697.
- 41 **Isenberg, G. and Klockner, U.,** Calcium tolerant ventricular myocytes prepared by preincubation in a "KB medium". *Pflugers Arch.* 1982. **395:** 6-18.

Figure Legends

Fig. 1

(A), Plasma Ig-Glu-tag protein (SP-Ig) and IL-13-Ig-Glu-tag protein (IL13-Ig) levels. The rats were injected with pCAGGS-rat SP-Ig-Glu-tag or pCAGGS-rat IL-13-Ig-Glu-tag on day 1. Chimeric protein concentrations were calculated by using Glu-tag. (B), IL-13-Ig-Glu-tag protein (IL13-Ig) levels calculated by using Glu-tag (●) or IL-13 ELISA (⊕). The Rats were injected with pCAGGS-rat IL-13-Ig-Glu-tag on day 7. Error bars represent SEM.

Fig. 2

(A) and (D), Heart weight/body weight ratio. (B) and (E), Myocarditis area in EAM heart. The area was calculated by a color image analyzer using specimens stained with Azan-Mallory. (C) and (F), Absolute copy numbers of ANP mRNA as a heart failure marker in EAM hearts. (A), (B) and (C), rats were injected with plasmid on day 1. (D), (E) and (F), rats were injected with plasmid on day 7. The rats were injected with pCAGGS-rat SP-Ig-Glu-tag (SP-Ig) or pCAGGS-rat IL-13-Ig-Glu-tag (IL-13-Ig). Error bars represent standard deviation. Statistical assessment was performed by a non-paired t-test.

Fig. 3

Histological examination of transverse sections in both ventricles of rats injected on day 1 were stained with Azan-Mallory stain. (A) and (C), transverse sections of the heart in SP-Ig group; (B) and (D), transverse sections of the heart in IL-13-Ig group. (C) and (D) were analyzed by a color image analyzer. Histological findings of rats injected on day 7 were similar to the above (data not shown).

Fig. 4

Infiltrating cells analyzed by immunohistochemistry in EAM hearts from SP-Ig group (n=9) and IL-13-Ig group (n=9). SP-Ig, rats were injected on day 1 with pCAGGS-rat SP-Ig-Glu-tag; IL13-Ig, rats were injected on day 1 with pCAGGS-rat IL-13-Ig-Glu-tag. (A), Total cells consisting of ED1⁺ cells, CD4⁺ cells and CD8⁺ cells per a

specimen of transverse heart sections. (B), ED1⁺ cells per total cells of transverse heart sections. (C), CD4⁺ cells per total cells of transverse heart sections. (D), CD8⁺ cells per total cells of transverse heart sections. Error bars represent SEM. Statistical assessment was performed by a non-paired t-test.

Fig. 5

Absolute copy numbers of IL-13R α 1 (A), IL-4R α (B), γ c (C), and IL-13R α 2 (D) mRNA. Each cell fraction (n=5) was separated and purified from an EAM heart on day 18. NCNI cells, non-cardiomyocytic non-inflammatory cells contain mainly fibroblasts, smooth muscle cells and endothelial cells. Error bars represent SEM. Statistical assessment was performed by one-way ANOVA and Bonferroni's multiple comparison test. Differences were considered significant at p<0.01. It was suggested that a small number of IL-4R α mRNA in $\alpha\beta$ T cell fractions was due to the contamination of CD11b⁺ cells and NCNI cells. We didn't guess that $\alpha\beta$ T cells expressed IL-13R α 1 mRNA.

Fig. 6

Copy numbers of various immunological molecules mRNA per copy numbers of γ actin mRNA in cultivated non-cardiomyocytic (NC) cells (n=6) in uncoated plates from EAM hearts. NC cells contain mainly fibroblasts, smooth muscle cells, endothelial cells and CD11b⁺ cells. (A), PGES; (B), Cox2; (C), iNOS; (D), IL-1 β ; (E), TNF α ; (F), IL-1RA; Negative control, cells were cultivated in medium containing neither IL-1 α nor rat serum; SP-Ig + IL-1, cells were cultivated in medium with IL-1 α and serum of a normal rat injected with pCAGGS-SP-Ig-Glu-tag; IL-13-Ig + IL-1, cells were cultivated in medium with IL-1 α and serum of a normal rat injected with pCAGGS-IL-13-Ig-Glu-tag. Final concentration of Ig-Glu-tag protein or IL-13-Ig-Glu-tag protein is 2 nmol/l. The concentration of IL-13-Ig-Glu-tag protein is similar to that in serum at early phase of EAM rat injected with pCAGGS-IL-13-Ig-Glu-tag on day 1 or day 7. Error bars represent SEM. Statistical assessment was performed by one-way ANOVA and Bonferroni's multiple comparison test. Differences were considered significant at p<0.01.

Fig. 7

Copy numbers of various immunological molecules mRNA per copy numbers of γ actin mRNA in cultivated non-cardiomyocytic (NC) cells (n=8) in uncoated plates from EAM hearts. (A), PGES; (B), Cox2; (C), iNOS; (D), IL-1 β ; (E), TNF α ; Negative control, SP-Ig + IL-1 and IL-13-Ig + IL-1 mean the same in Fig.6. Final concentration of Ig-Glu-tag protein or IL-13-Ig-Glu-tag protein is 1 nmol/l. The concentration of IL-13-Ig-Glu-tag protein is similar to that in serum at climax of EAM rat injected with pCAGGS-IL-13-Ig-Glu-tag on day 7. Expressions of IL-1RA were not significantly different among the groups (data not shown). Error bars represent SEM. Statistical assessment was performed by one-way ANOVA and Bonferroni's multiple comparison test. Differences were considered significant at $p < 0.01$.

Table 1. Absolute copy numbers of specific cell marker mRNA
in cultivated NC cells

	copy numbers of mRNA/ μ g of total RNA NC cells (n=6)
CD3	19,100 \pm 12,100
collagen type III	228,000,000 \pm 91,800,000
calponin	2,220,000 \pm 1,090,000
CD11b	4,330,000 \pm 1,670,000
von Willebrand factor	82,300 \pm 36,700
α cardiac myosin	N. D.

Results are expressed as the mean \pm SEM N. D. : not detected.
These cells were used in the experiment of Fig. 6

Table 2. List of Primers for quantitative RT-PCR

	Sense Primer	Antisense Primer
ANP	5'-atggatttcaagaacctgctagac-3'	5'-gctccaatcctgtcaatcctac-3'
α cardiac myosin	5'-acaaggttaaaaacctgacagagg-3'	5'-tactgttctgctgactgatgtcaa-3'
CD3	5'-gatccaaactctgctatatgcta-3'	5'-ctttcatgccaatctcactgtag-3'
CD11b	5'-gggatccgtaaagtagtgagaa-3'	5'-aaaggagctggacttctctct-3'
collagen type III	5'-cgcaattgcagagacctgaa-3'	5'-acagtcatgggactggcatttat-3'
von Willebrand factor	5'-agaggctacacatctctcagaagc-3'	5'-gacctttttttttgaaaccttg-3'
calponin	5'-aacataggaaatttcatcaaagcc-3'	5'-gtagactgatagtgcctgatcca-3'
IL-13R α 1	5'-gaagcgtgagatagtaaggag-3'	5'-ccgctttcttaggttttctatca-3'
IL-13R α 2	5'-ctatgtttttctggtatgagggt-3'	5'-aatatcatcttctcggaccacaat-3'
IL-4R α	5'-taccggagtttagtgacttctcc-3'	5'-gagaaagccttgtaaccagtgtct-3'
γ c chain	5'-tgccatctagatccttcttactcc-3'	5'-tcttttgagaacagatagtggtg-3'
PGES	5'-gtgatggagaacagccagg-3'	5'-gaggaccacgaggaaatgtatc-3'
Cox2	5'-tgtgatattctcaaacaggagcat-3'	5'-aaggaggatggagttgttagag-3'
iNOS	5'-ttctactattaccagatcgagccc-3'	5'-gtagttgttctcttccaaggtgt-3'
IL-1 β	5'-gctagtgtgatgttccattag-3'	5'-cttttccatcttcttctttggta-3'
TNF α	5'-atgggtccctctcatcagt-3'	5'-actccagctgctcctctgct-3'
IL-1RA	5'-agaagaaaagatagacatggtgcc-3'	5'-actttgtgactgtacaggctctt-3'
γ -actin	5'-agccttcttctctgggcatggagt-3'	5'-tggagggcctgactcgtcact-3'

Fig. 1.

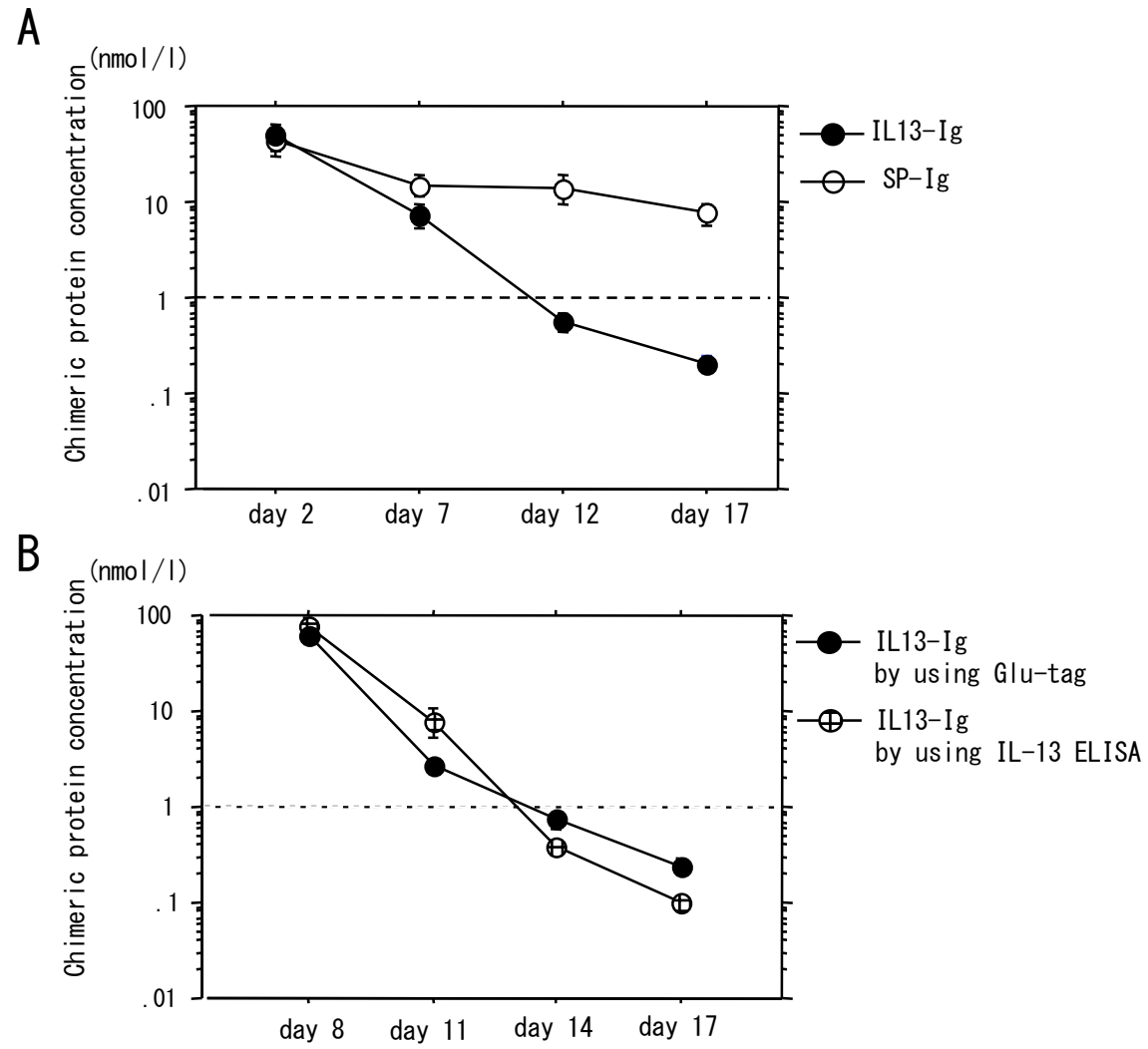


Fig. 2.

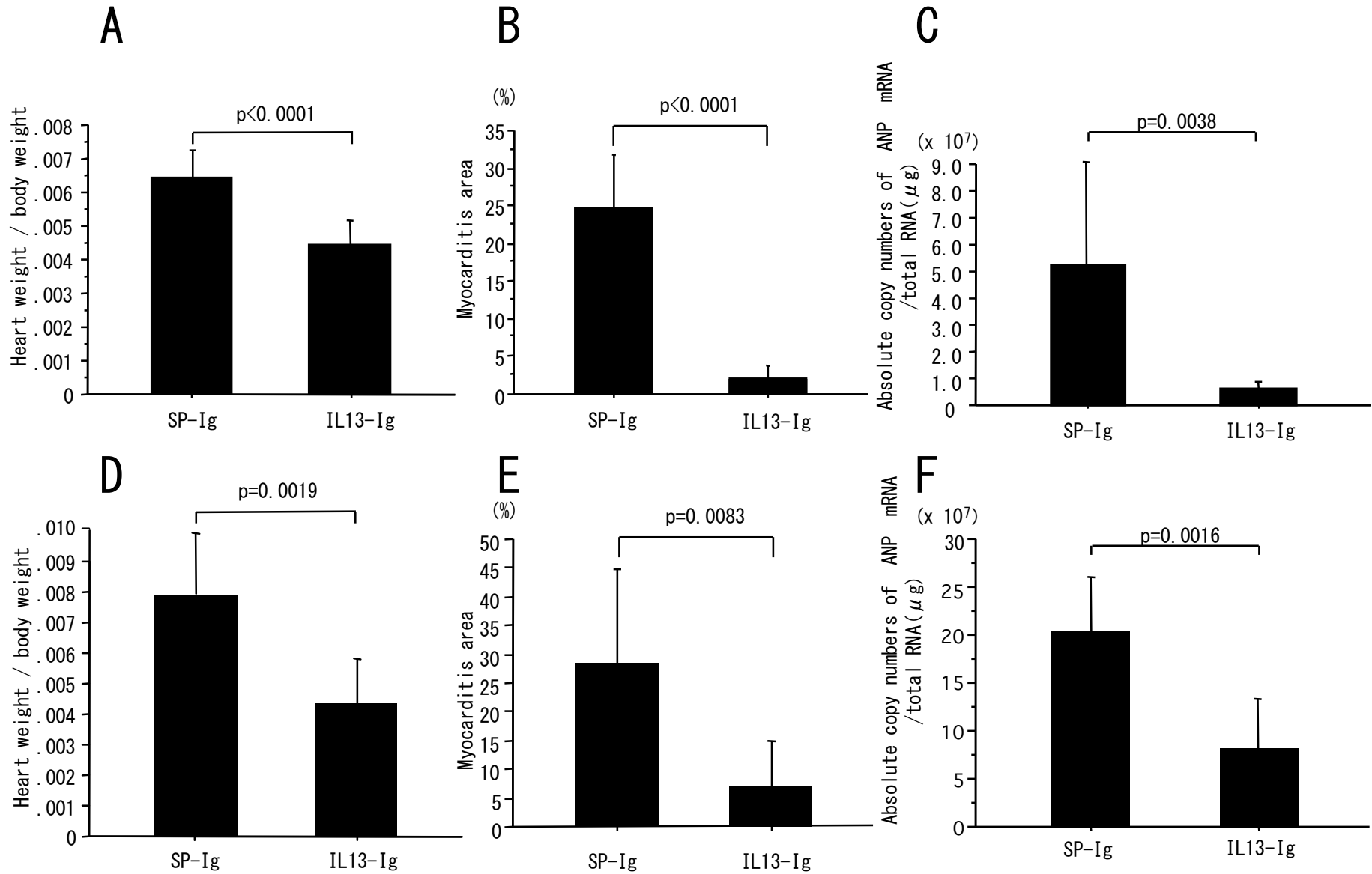


Fig. 3.

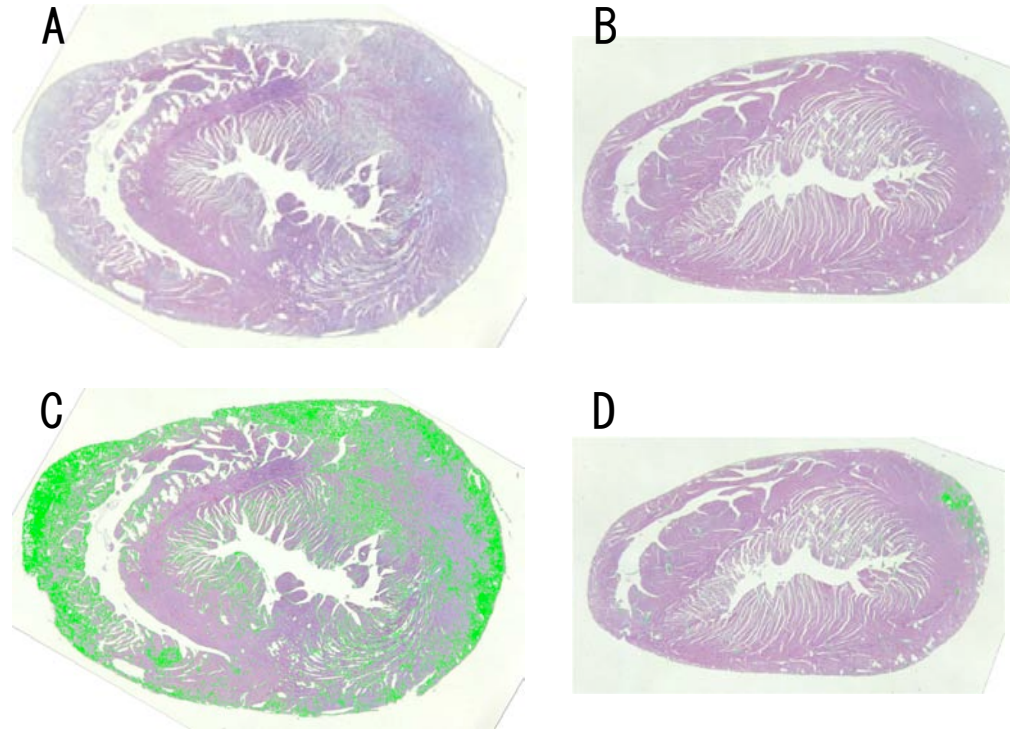


Fig. 4.

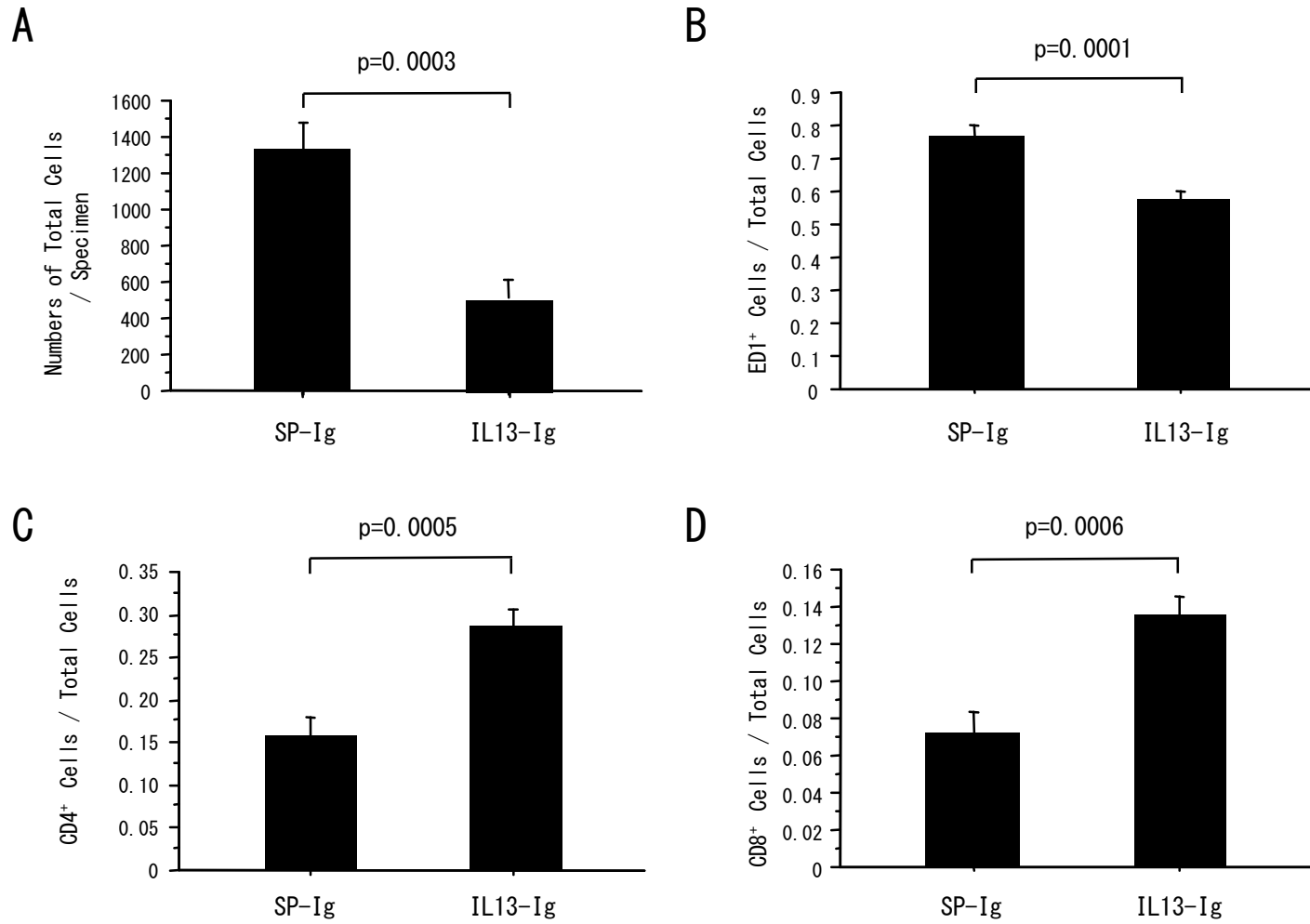


Fig. 5.

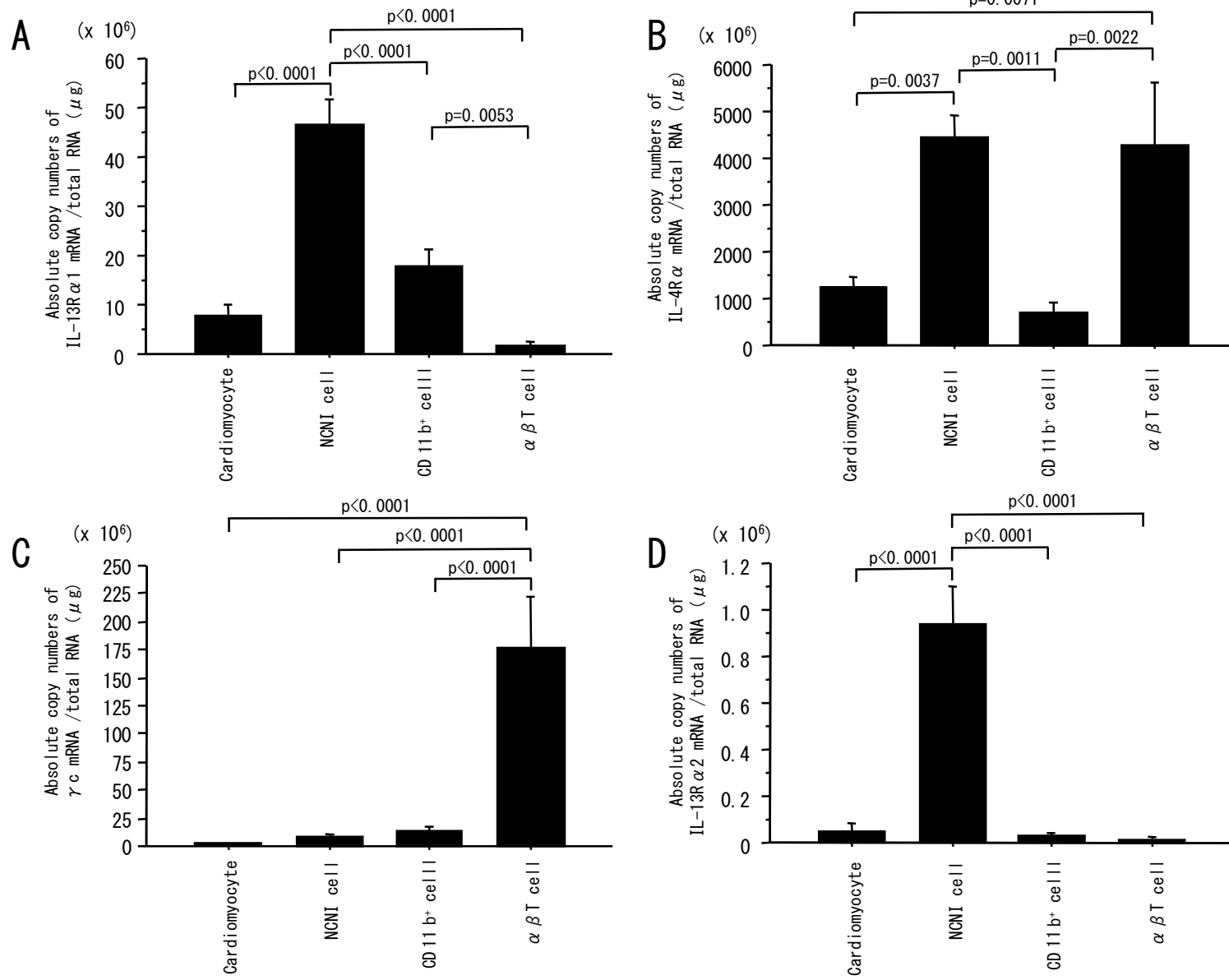


Fig. 6.

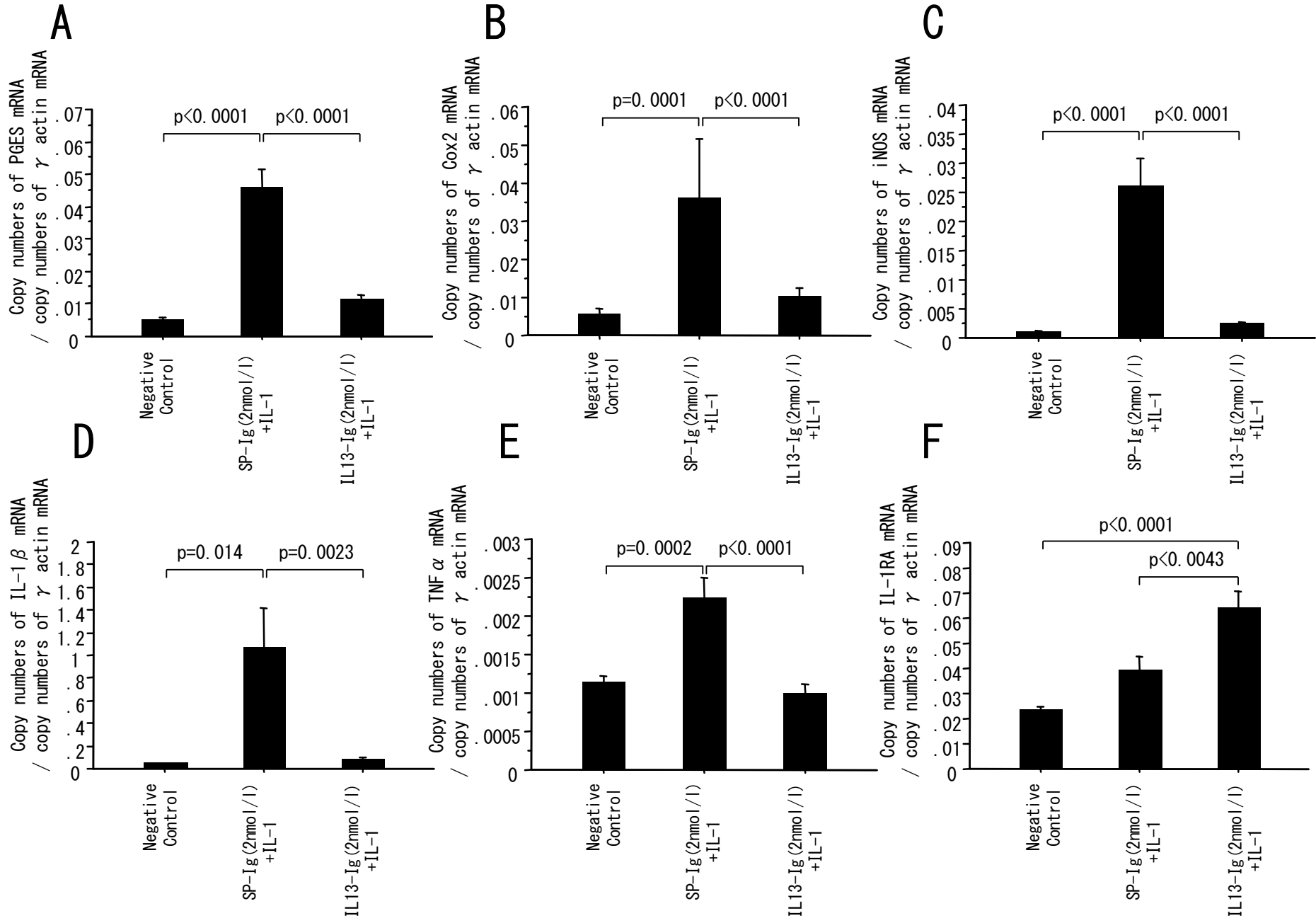


Fig. 7.

